AMERICAN SOCIETY of
GENE & CELL
THERAPY

lncRNA GCAWKR Promotes Gastric Cancer Development by Scaffolding the Chromatin Modification Factors WDR5 and KAT2A

Mingzhe Ma,[1,2,8] Yan Zhang,[3,8] Mingzhe Weng,[4,8] Ye Hu,[5] Yi Xuan,[1,2] YiRen Hu,[6] and Kun Lv[7]

[1]Department of Gastric Surgery, Fudan University Shanghai Cancer Center, Shanghai, China; [2]Department of Oncology, Shanghai Medical College, Fudan University, Shanghai, China; [3]Department of Gastroenterology, Yijishan Hospital, The First Affiliated Hospital of Wannan Medical College, Wuhu, Anhui, China; [4]Department of General Surgery, Xinhua Hospital, Shanghai Jiaotong University School of Medicine, Shanghai, China; [5]State Key Laboratory for Oncogenes and Related Genes, Division of Gastroenterology and Hepatology, Ren Ji Hospital, Shanghai Jiao Tong University School of Medicine, Shanghai, China; [6]Department of General Surgery, Wenzhou No. 3 Clinical Institute of Wenzhou Medical University, Wenzhou People's Hospital, Wenzhou, Zhejiang, China; [7]Central Laboratory of Yijishan Hospital, The First Affiliated Hospital of Wannan Medical College, Wuhu, Anhui, China

Long noncoding RNAs (lncRNAs) have been demonstrated to play a role in carcinogenesis, but their mechanisms of function remain elusive. We explored the mechanisms of the oncogenic role of *GCAWKR* in gastric cancer (GC) using human tissues and cell lines. The *in situ* hybridization analysis was utilized to determine *GCAWKR* levels in samples from 42 GC patients and real-time qPCR in tissues from 123 patients. The *GCAWKR* levels were modulated in GC cell lines, and relevant biological and molecular analyses were performed. Levels of the *GCAWKR* were upregulated in GC tissues compared with normal tissues and associated with tumor size, lymph node metastasis, TNM stage, and patient outcomes. *GCAWKR* affected cell proliferation and cell invasion in multiple GC models. Mechanistically, *GCAWKR* bound WDR5 and KAT2A and acted as a molecular scaffold of WDR5/KAT2A complexes, modulating the affinity for WDR5/KAT2A complexes in the target gene's promoter region. Thus, our data defined a mechanism of lncRNA-mediated carcinogenesis in GC, suggesting new therapeutic targets in GC.

INTRODUCTION

Gastric cancer (GC) is the fourth most common cancer by incidence and the third leading cause of cancer death worldwide.[1,2] Although great advances have been made in the diagnosis and management of GC, the prognosis of GC patients remains dismal, especially for patients at advanced stages. Tumor recurrence, metastasis, and therapy resistance are the main causes of cancer-related death.[3] Although a growing number of studies have tried to clarify the pathophysiological mechanisms of GC progression and the development of early GC diagnostic and prognostic biomarkers, the improvement in the prognosis of GC patients at advanced stages is considered unsatisfactory.[4] Therefore, more efforts are required for the development of novel biomarkers and targets for GC diagnosis and therapy.

Long noncoding RNAs (lncRNAs) are a class of noncoding RNAs longer than 200 nucleotides in length and with no protein-coding po-

tential.[5] Accumulating evidence has demonstrated that lncRNAs play an important role in a wide array of cellular processes, including carcinogenesis.[6–8] lncRNAs have been reported to regulate genes at multiple levels, including transcriptional modulation by recruiting chromatin-modifying complexes[9] and post-transcriptional regulation by interacting with microRNAs (miRNAs),[10] mRNAs,[11] or proteins.[12] Although there have been up to 548,640 lncRNAs that have been annotated according to NONCODE V5,[13] only a small portion of them have been functionally characterized.

In the present study, we analyzed our previous genome-wide lncRNA profiling data in GC tissues and paired normal tissues.[14] We characterized a novel lncRNA (ENST00000431060). The biological functions of the gastric-cancer-associated WDR5 and KAT2A binding lncRNA (lncRNA-*GCAWKR*) was determined in the *in vitro* and *in vivo* models.

RESULTS

lncRNA *GCAWKR* Was Upregulated in GC Tissues

The lncRNA and mRNA profiling data in 10 GC and paired normal tissues that we previously reported[14] can be accessed via Gene Expression Omnibus (GEO): GSE50710. We analyzed the microarray data and used stringent filtering criteria (fold change >2, $p < 0.05$, raw
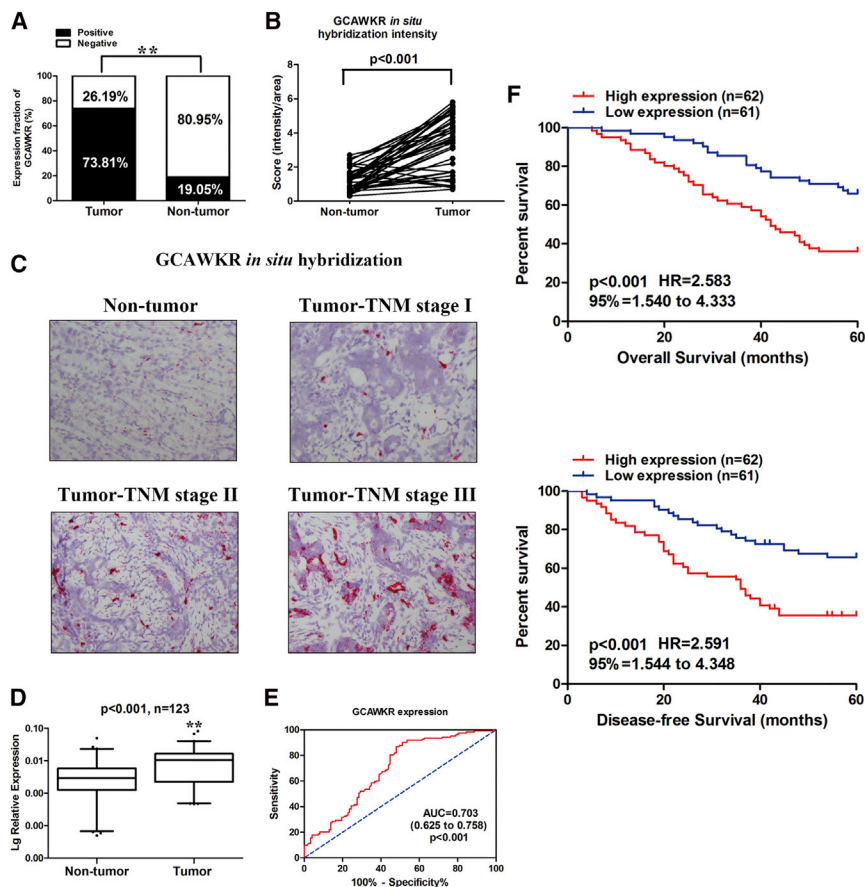
Figure 1. *GCAWKR* Upregulation in GC Tissues

(A) *GCAWKR* expression in GC tissues and adjacent nontumor tissues was determined in ISH assays (cohort 1, n = 42). **p < 0.01. (B) Statistical analysis of *GCAWKR* expression in 42 paired normal and cancerous gastric tissues. The y axis indicates staining intensity of *GCAWKR*. The expression level of *GCAWKR* was significantly higher in cancerous tissues (p < 0.0001, paired t test). (C) ISH of *GCAWKR* in normal gastric mucosa or gastric cancer tissues. Paraffin-embedded tissue sections were stained using specific probe for *GCAWKR*. The expression level of *GCAWKR* was higher in tissues with advanced TNM stage. (D) *GCAWKR* expression was analyzed by qRT-PCR in GC samples and adjacent nontumor tissues (cohort 2, n = 123). *GCAWKR* expression level was normalized to that of β-actin. Horizontal lines in the boxplots represent the medians, the boxes represent the interquartile range, and the whiskers represent the 2.5th and 97.5th percentiles. The significant differences between samples were analyzed using the Wilcoxon signed-rank test. **p < 0.01. (E) ROC curve for prediction of gastric cancer using qRT-PCR-based *GCAWKR* expression level. The AUC was 0.703, with 95% CI and p value indicated. (F) Kaplan-Meier survival analysis of overall survival (OS) and disease-free survival (DFS) in GC patients (p < 0.001 for both OS and DFS) based on *GCAWKR* expression.

signal intensity >1,000). Bioinformatics analysis found that the level of lncRNA-*GCAWKR* was higher in GC tissues than that in normal tissues. *GCAWKR* (linc-ALDH1A3-1, LNCipedia annotation; NONHSAT051130, NONCODE v4; ENST00000431060, Ensembl release 64, Sep 2011) was on human chromosome 15:101390036–101404487. *GCAWKR* consists of five exons and spanned about 3,900 bp. The 5′ and 3′ rapid amplification of cDNA ends (RACE)-PCR was performed to identify the 5′ and 3′ ends of *GCAWKR* (Figure S1). Then, we evaluated the potential coding capability of *GCAWKR*; the results were as follows: although seven short open reading frames (ORF1, 3, 8, 9, 11, 12, and 13) with more than 200 nt were predicted using ORF Finder from the National Center for Biotechnology Information (Figure S2A); none of their AUGs showed the Kozak consensus and no homologous protein sequences were found using a BLAST search; The online protein-coding potential assessment softwares (coding potential calculator; coding potential score, −0.870037; PhyloCSF, codon substitution frequency scores, −15.3106) (Figure S2B) and *in vitro* translation assays (Figure S2C) also confirmed *GCAWKR* has no coding capability. We separated the cytoplasm and nuclear fractions of GC cell lines (SGC7901 and BGC823 cells) and performed PCR analysis. *GCAWKR* was mainly located in the nucleus of GC cells (Figure S2D). We found that the expression

of *GCAWKR* was upregulated in GC cell lines compared to normal human gastric epithelial cell line (GES-1) (Figure S3A). The expression level of *GCAWKR* was comparable to the well-known oncogenic lncRNA *MALAT1* (Figure S3B). The predicted secondary structures image with ViennaRNA is presented in Figure S3C.

As human *GCAWKR* consists of three transcripts (*GCAWKR* 1–3; Figure S4A), we examined the expression levels of all *GCAWKR* transcripts in GC cell lines. Only the *GCAWKR*-1 was highly expressed of GC cell lines and GC tissues, while *GCAWKR*-2 and −3 were barely detected in GC cell lines, GC tissues, and adjacent normal tissues (Figures S4B and S4C).

lncRNA *GCAWKR* Correlated with GC Progression

qRT-PCR analysis demonstrated that the expression level of *GCAWKR* increased from normal gastric tissue to intestinal metaplasia (IM), to dysplasia, and to GC (Figure S5A). The expression level of *GCAWKR* was upregulated in GC tissues compared to adjacent normal tissues in another GC dataset from the GEO database (Figure S5B). There was no difference in the expression level of *GCAWKR* between *Helicobacter pylori*-positive and -negative GC tissues (Figure S5C). *In situ* hybridization (ISH) of 42 paraffin-embedded GC cancer tissues and adjacent normal tissues (Table S3, cohort 1) confirmed that *GCAWKR* was upregulated in GC tissues (Figures 1A and 1B) and higher expression of *GCAWKR* was more
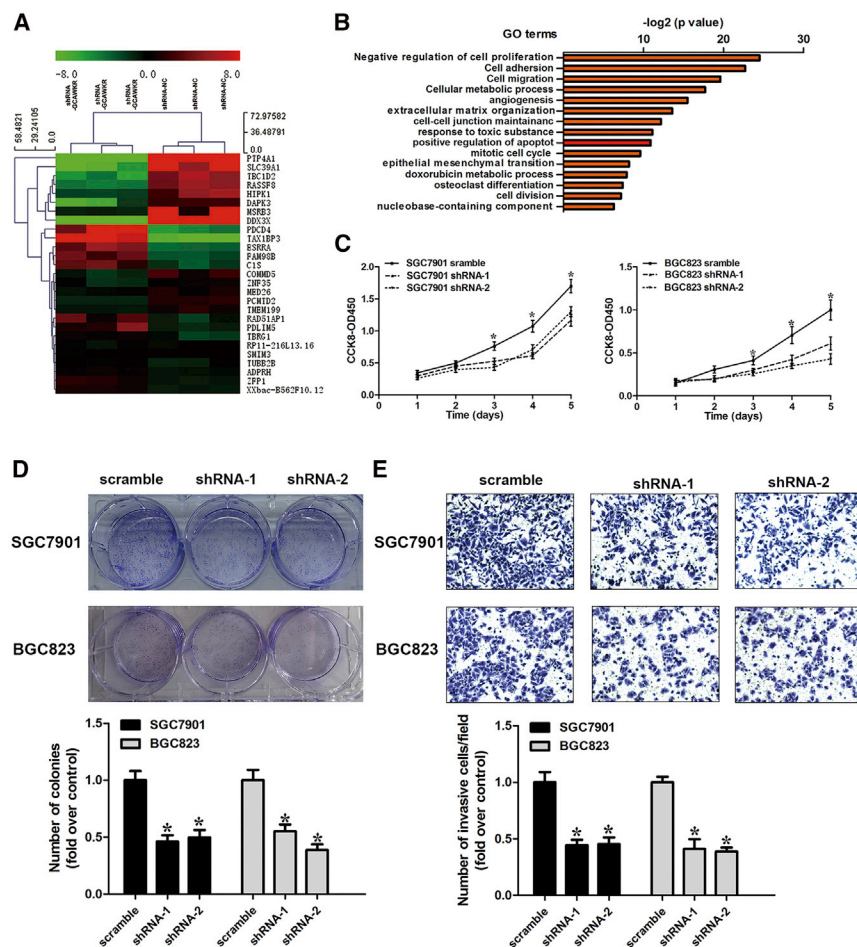
average ΔCt expression value of 5.675, ranking from 3.649 to 6.545) was classified as values ≥ median ratio. The high-*GCAWKR*-expression group demonstrated a larger tumor size (p = 0.012) and advanced lymph node status (p = 0.016), depth of invasion (p = 0.045), and TNM stage (p = 0.031) (Table S4). High *GCAWKR* expression was associated with a poorer overall survival (OS) (p < 0.001; Figure 1F) and disease-free survival (DFS) (p < 0.001; Figure 1F). Univariate and multivariate Cox proportional hazards analysis showed that *GCAWKR*, depth of invasion, and TNM stage were independent factors for OS in GC patients (Table S5). *GCAWKR* and TNM stage were identified to be independent prognostic factors for DFS in GC (Table S6).

frequent in tissues with advanced tumor-node-metastasis (TNM) stage (Figure 1C). As shown in Table S3, a positive correlation among *GCAWKR* expression and tumor size (p = 0.023), advanced American Joint Committee on Cancer (AJCC) TNM stage (p = 0.028), lymph node status (p = 0.002), and gross type (p = 0.048) was found. To further investigate the role of *GCAWKR* in GC, we determined the transcript levels of *GCAWKR* in 123 pairs of GC tissues and adjacent normal tissues. We found that *GCAWKR* was upregulated in 78.86% (97/123) GC tissues compared to matched adjacent normal tissues (Figure 1D). Furthermore, we utilized the receiver operating characteristic (ROC) curves to assess the predictive power of *GCAWKR* expression in differentiating GC tissues from normal tissues. It is worth noting that *GCAWKR* manifested itself with considerable predictive significance, with an area under the curve (AUC) of 0.703 (95% confidence interval [CI], 0.625–0.758; p < 0.001; Figure 1E). The median *GCAWKR* expression level was used as the cutoff value. Low *GCAWKR* expression levels in 61 patients (with an average ΔCt expression value of 8.842, ranking from 6.560 to 11.093 when compared with β-actin) was classified as values < median ratio. High *GCAWKR* expression in 62 patients (with an

GCAWKR Promotes GC Progression, and PTP4A1 Is a Downstream Target of GCAWKR

To explore the biological function of *GCAWKR* on the progression of GC, we next performed loss-of-function and gain-of-function studies in GC cells. After detecting *GCAWKR* expression in five GC cell lines (Figure S3A), we selected SGC7901 and BGC823 cells lines for manipulation of *GCAWKR* expression (Figures S6A–S6D), as they had moderate expression levels of *GCAWKR*. To elucidate the potential role involved in the oncogenic function of *GCAWKR*, an RNA transcriptome-sequencing analysis was performed in SGC7901 cells that were transfected with *GCAWKR* short hairpin RNA (shRNA) or control shRNA (Figure 2A; data are available via GEO: GSE112586). Top altered cellular pathways were the negative regulation of cell proliferation, cell adhesion and cell migration (Figure 2B). These genes (proliferation-related genes, CDK1, CDC25B, CCND3, and GDF13; migration-related genes, KLF6, MMP9, MAPK4, and HOXB13) were selectively confirmed by qRT-PCR analysis (Figures S6E
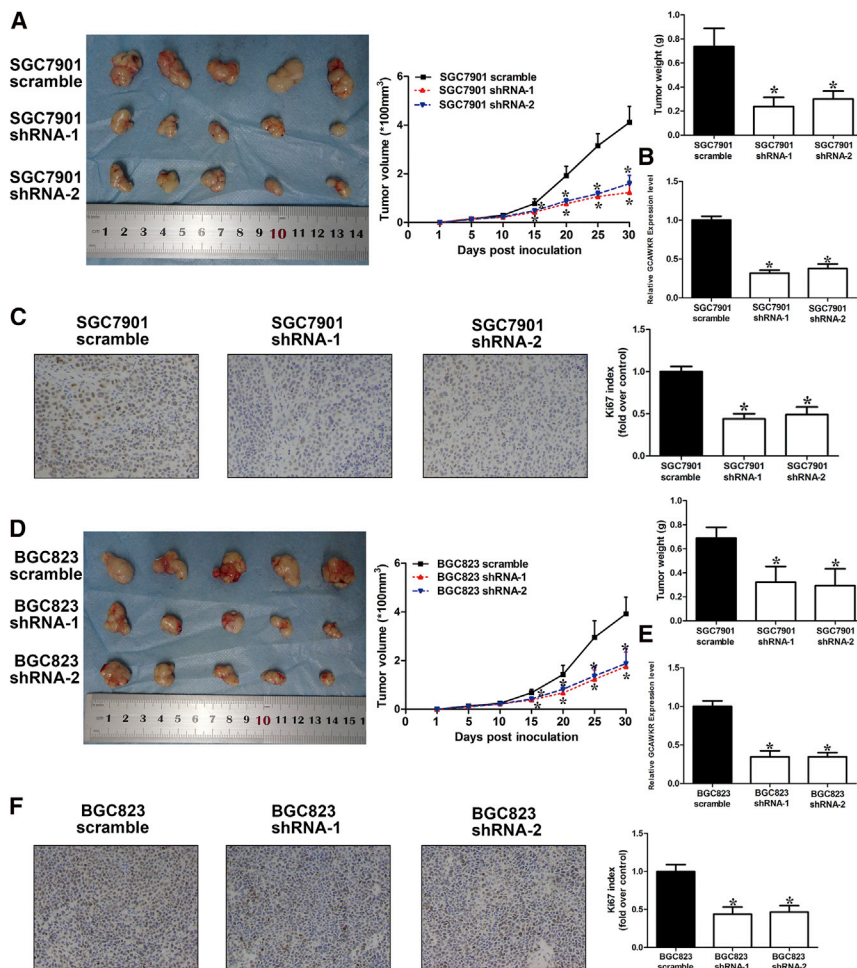
Figure 3. Knockdown of *GCAWKR* Inhibited Tumor Growth *In Vivo*

(A and D) Top left, representative images of tumors formed in nude mice injected subcutaneously with *GCAWKR*-silencing SGC7901 cells (A) or BGC823 cells (D) (n = 5 per group). Top middle, tumor growth curves. Top right, tumor weights. (B and E) *GCAWKR* levels were determined in tumors from mice with qRT-PCR in SGC7901 (B) and BGC823 cells (E). (C and F) Representative images of IHC staining of Ki67 in SGC7901 (C) and BGC823 cells (F) (original magnification, ×200). *$p < 0.05$.

The oncogenic function of *GCAWKR* was further confirmed in the xenograft mouse tumor models. Knockdown of *GCAWKR* significantly suppressed tumor growth, as illustrated by decreased tumor growth rates, tumor weights, and Ki-67 indexes from the *GCAWKR*-downregulated xenografts compared with that of tumors from the control xenografts (Figures 3A–3F), while *GCAWKR* overexpression promoted tumor growth (Figures S8B–S8E). These data suggest that *GCAWKR* promoted GC cell progression.

Among the differentially expressed genes (SGC7901 cells that were transfected with shRNA-GCAWKR versus shRNA-negative control [NC]), PTP4A1 (protein tyrosine phosphatase type IVA, member 1), located in 6q129, is associated with poor clinical prognosis and could promote cell growth and invasion in cancer.[15–17] Furthermore, PTP4A1 was significantly overexpressed in 100% of gastric carcinomas[18] (Figure S9A) and a variety of cancer tissues (Figure S9B). Immunohistochemical staining analysis confirmed that PTP4A1 was upregulated in GC tissues compared to normal tissues (Figure S9C). A higher expression level of PTP4A1 is correlated with a significantly poorer disease-specific survival (DSS; $p < 0.05$) and DFS ($p < 0.05$) according to data from the KMPlot database (http://www.kmplot.com) (Figures S10A and S10B). A positive correlation between *GCAWKR* and PTP4A1 transcript levels was found in 35 GC patients (cohort 2, $r^2 = 0.461$, $p < 0.001$; Figure 4A). Therefore, we chose PTP4A1 for further investigation. qRT-PCR and western blot analysis showed that *GCAWKR* silencing markedly decreased the expression levels of PTP4A1 (Figure 4B), while *GCAWKR* overexpression increased the expression levels of PTP4A1 in SGC7901 and BGC823 cells (Figure 4C). To determine the regulatory effect of *GCAWKR* on the transcriptional activity of PTP4A1, we cloned the 5′ flanking DNA fragment (~2 kbp) of PTP4A1 promoter region and inserted it into pGL3 enhancer plasmid. Luciferase activity of pGL3 enhancer plasmid was significantly decreased with *GCAWKR* silencing in SGC7901 and BGC823 cells (Figure 4D). It suggests that *GCAWKR* might promote the transcription of PTP4A1 in GC.

and S6F). These data suggest that *GCAWKR* may play a role in the development of GC.

Cell-counting kit-8 and colony-formation assays demonstrated that knockdown of *GCAWKR* suppressed the proliferative capacity in SGC7901 and BGC823 cells (Figures 2C and 2D). Conversely, overexpression of *GCAWKR* promoted cell proliferation *in vitro* (Figures S7A and S7B). *GCAWKR*-knockdown GC cells had a significantly higher percentage of Annexin V-positive cells than did cells expressing a scrambled shRNA (Figure S7C). Furthermore, knockdown of *GCAWKR* increased the sensitivity to chemotherapeutics (Figures S7D and S7E). Then, we performed the transwell assays to investigate the effect of *GCAWKR* on GC cell invasive ability. To prevent cell number changes that could potentially affect the outcome of the assays, the transwell assays were performed in the presence of mitomycin C (MMC), which is an anti-proliferative drug. The results demonstrated that the invasive ability in SGC7901 and BGC823 cells was decreased when *GCAWKR* expression was knocked down (Figure 2E), while *GCAWKR*-overexpressing SGC7901 and BGC823 cells exhibited higher invasive ability (Figure S8A).
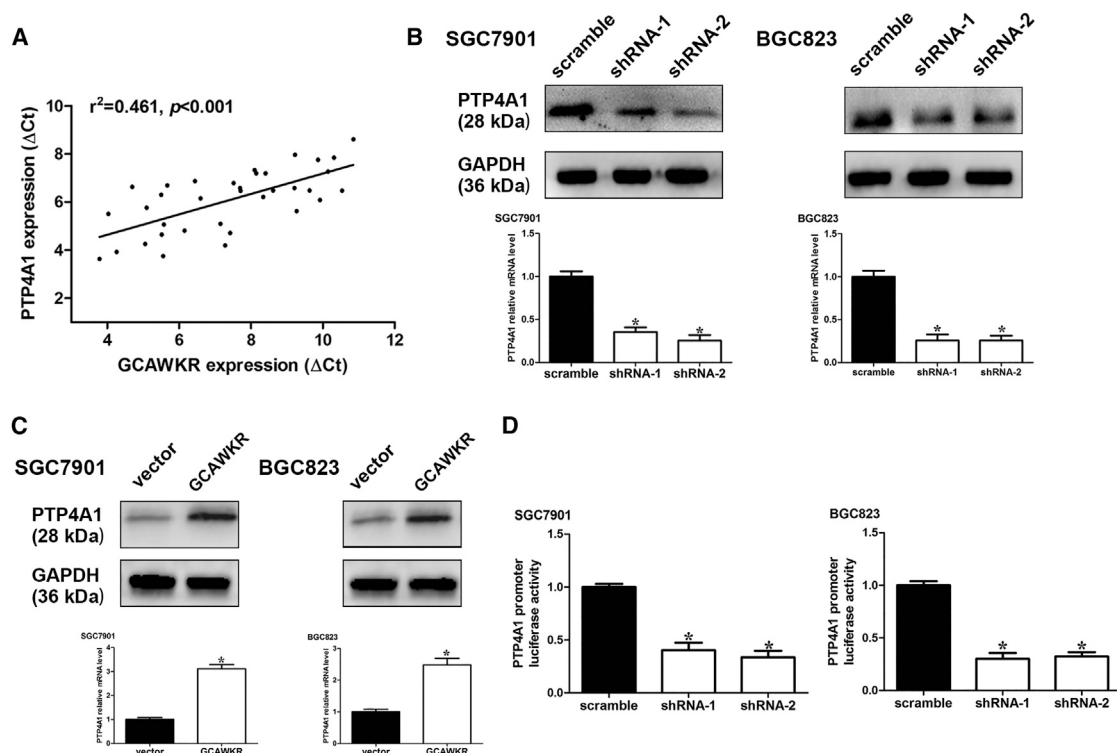
Figure 4. *GCAWKR* Correlates With and Regulates PTP4A1

(A) The correlation between *GCAWKR* transcript level and PTP4A1 mRNA level was measured in 35 GC tissues. The ΔCt values (normalized to β-actin) were subjected to Spearman rank-correlation analysis. (B) qRT-PCR and western blot assays were performed in SGC7901 and BGC823 cells after transfection of *GCAWKR* shRNAs. n = 3, nonparametric Mann-Whitney test. Error bars in the bar graphs represent SD. (C) The PTP4A1 expression was detected with real-time PCR and western blot in SGC7901 and BGC823 cells after transfection of lentivirus harboring the full-length human *GCAWKR* sequence or the empty vector. (D) Luciferase reporter vector was generated by inserting the promoter region (−2,000 to 0 bp) of the PTP4A1 gene. The reporter vectors were then cotransfected into SGC7901 and BGC823 cells with *GCAWKR* or control shRNAs. Cells were harvested for luciferase activity assay. Results shown are the mean ± SD of triplicate determination from three independent experiments. *p < 0.05.

GCAWKR Functions as a Scaffold for WDR5 and KAT2A in the Nucleus and Thus Epigenetically Upregulates PTP4A1

Previous reports have demonstrated that a part of lncRNAs function via scaffolding chromatin modifier to facilitate epigenetically modulation of gene expression.[19] As *GCAWKR* was mainly located in the nucleus, the interaction probabilities of *GCAWKR* and a panel of RNA binding proteins, including HuR, Ago, STAU1, TDP-43, EZH2, SUZ12, SUV39H1, LSD1, SIRT1, DNMT1, CoREST, DNMT3a, DNMT3b, SETDB1, WDR5, HAT1(KAT1), GCN5(KAT2A), PCAF(KAT2B), CBP(KAT3A), and p300(KAT3B) were predicted via the online RNA-Protein Interaction Prediction Program (Figure S11A). We found that *GCAWKR* potentially interacts with WDR5 and KAT2A (more stringent filtering criteria, reading frame (RF), and support vector machine [SVM] score > 0.5). RNA pull-down assay (Figure 5A) confirmed that *GCAWKR* specifically binds to WDR5 and KAT2A. WDR5, a key component of SET/MLL (SET-domain/mixed-lineage leukemia) histone-methyltransferase complexes, have an essential role in histone H3 Lys 4 (H3K4) trimethylation and subsequent transcriptional activation.[20] KAT2A (GCN5), a histone acetyltransferase, modulates histone H3K9 acetylation levels and gene transactivation.[21] Reports have shown that

lncRNAs could function as scaffold for RNA-binding proteins.[22,23] As WDR5 and KAT2A exert oncoepigenic effects in tumorigenesis,[24–26] we speculated that *GCAWKR* might coordinately interact with WDR5 and KAT2A. We found that the binding activity mapped to 3′ end segment (nucleotides 3,000–3,893) of *GCAWKR* (Figure 5B). The 3′ end segment formed a stable stem-loop structure according to RNA folding analyses[27] (Figure S11B), which may provide the spatial conformation for the interaction. Furthermore, the effect that knockdown of *GCAWKR* had on the protein levels of WDR5 and KAT2A was not significant (Figure S11C). To further consolidate the interaction, we analyzed the interaction between *GCAWKR* and WDR5/KAT2A in the nucleus, and the radioimmunoprecipitation (RIP) assays showed that *GCAWKR* specifically binds to WDR5 and KAT2A (Figure 5C). Significant enrichment of *GCAWKR* was observed in the anti-WDR5 and anti-KAT2A immunoprecipitates compared with GAPDH (Figure S11D). These data suggests that *GCAWKR* might serve as a scaffold and specifically binds with WDR5 and KAT2A in GC. In addition, coimmunoprecipitation (coIP) assays demonstrated that WDR5 retrieved KAT2A and KAT2A retrieved WDR5 (Figure 5D), which suggests that WDR5 and KAT2A physically bind with each other. *GCAWKR* silencing
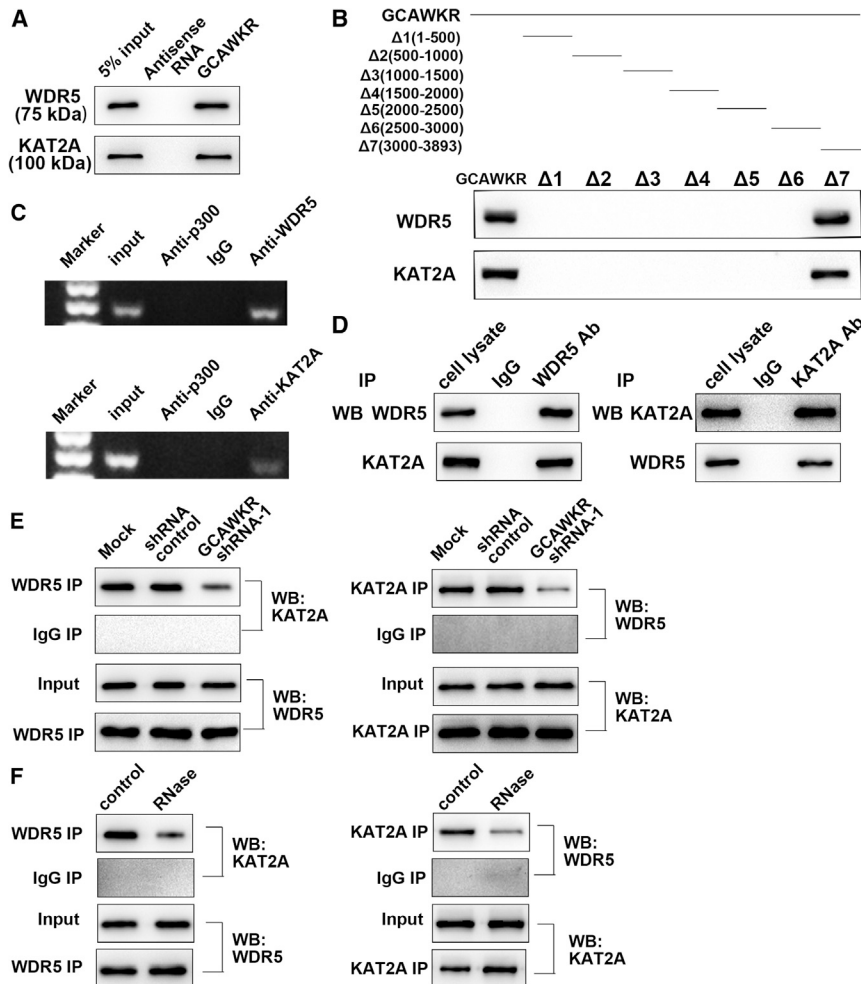
Figure 5. *GCAWKR* Interacts with WDR5 and KAT2A

(A) Biotinylated GCAWKR or antisense RNA was incubated with cell extracts of SGC7901 cells, targeted with streptavidin beads, and washed, and the associated proteins were resolved on a gel. Western blot analysis detected the specific association of WDR5 or KAT2A and GCAWKR (n = 3). (B) Biotinylated RNAs corresponding to different fragments of GCAWKR were incubated with SGC7901 cell lysates, and associated proteins were resolved electrophoretically. Western blot analysis of the specific association of WDR5 or KAT2A and GCAWKR (n = 3). (C) RIP experiments were performed using the WDR5, KAT2A, or p300 antibody for immunoprecipitation and a primer to detect GCAWKR. RIP enrichment was determined relative to the input controls (n = 3). (D) Coimmunoprecipitation detected the interaction between WDR5 and KAT2A in SGC7901 cells. The 20% of input and WDR5 or KAT2A immunoprecipitates were separated by SDS-PAGE. The interaction between WDR5 and KAT2A was confirmed by western blot (n = 3). (E and F) Immunoprecipitation assays were used to determine the interaction between WDR5 and KAT2A after transfection of GCAWKR shRNA (E) or RNase treatment (F). n = 3. For RNase treatment, cells were treated with RNase A (100 μg/mL) at 37°C for 1 hr.

(Figure 5E) or RNAase treatment (Figure 5F) greatly suppressed the interaction between WDR5 and KAT2A. Our data illustrated that *GCAWKR* mediated the interaction between WDR5 and KAT2A.

To determine whether histone acetylation is involved in PTP4A1 transcription, we found that the treatment of Trichostatin A (an inhibitor of class I and II histone deacetylases) induced a significant upregulation of PTP4A1 in SGC7901 and BGC823 cells (Figure S12A). To determine which group of histone acetyltransferases (HATs) (HATs can be classified into five groups: EP300/CREBBP, basal transcription factors, MYST, GNAT, and nuclear receptor cofactors)[21] might be involved in the transcription of PTP4A1, we treated GC cells with three pharmacological HAT inhibitors: CPTH2 (an inhibitor of KAT2A network), curcumin (an inhibitor of EP300/CREBBP), and anacardic acid (an inhibitor of both EP300 and PCAF). We found that CPTH2 abolished the increase in luciferase activity of pGL3 enhancer plasmid of PTP4A1 induced by *GCAWKR* overexpression in BGC823 cells (Figure S12B), which suggests that KAT2A might play a role in this process. To further consolidate the hypothesis, we performed western blot analysis and found that WDR5 or

KAT2A knockdown (Figure S12C) obviously attenuated the *GCAWKR*-induced PTP4A1 upregulation in SGC7901 (Figure 6A) and BGC823 cells (Figure S12D). It indicates that WDR5 and KAT2A are involved in the coregulation of PTP4A1. Furthermore, WDR5, KAT2A, or *GCAWKR* silencing obviously inhibited the luciferase activity of pGL3 enhancer plasmid of PTP4A1 (Figure 6B). The chromatin IP (ChIP) assay confirmed the binding of WDR5 and KAT2A to the promoter region of PTP4A1 (Figure 6C). *GCAWKR* silencing markedly suppressed the binding ability of WDR5 and KAT2A (Figure 6D). In addition, we observed the significant enrichment of H3K9ac and H3K4me3 at the promoter region of PTP4A1 (Figure 6E). GCAWKR silencing induced obvious decreased H3K9ac and H3K4me3 levels at the promoter region of PTP4A1 (Figure 6F). These results suggest that *GCAWKR* serves as a molecular scaffold for WDR5 and KAT2A and activate the transcription of PTP4A1.

GCAWKR Promotes GC Development by Upregulating PTP4A1 Expression

Next, we would like to investigate whether PTP4A1 modulates the biological function of *GCAWKR* in GC. *GCAWKR* overexpression significantly promoted the GC cell proliferation (Figure 7A), colony formation (Figure 7B), and invasion (Figure 7C) in GC cells, and PTP4A1 knockdown (Figure S13A) attenuated the oncogenic effect induced by the *GCAWKR* overexpression. Furthermore, the growth of tumors from *GCAWKR*-overexpressing xenografts was blocked by the downregulation of PTP4A1 (Figure 7D). On the contrary,
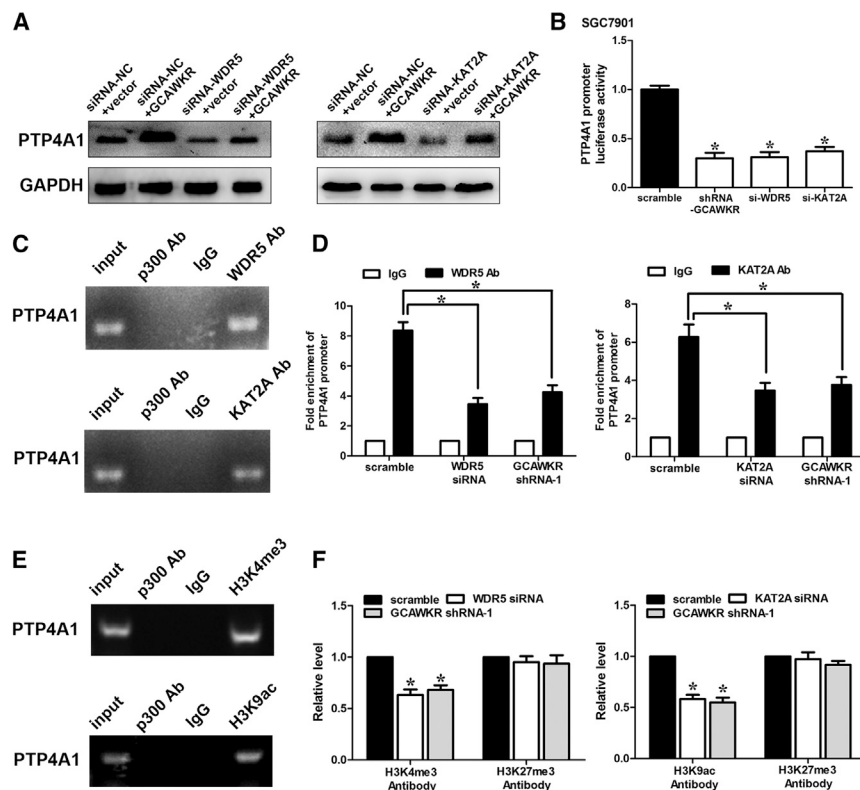
Figure 6. *GCAWKR* Functions as a Link between WDR5/KAT2A and PTP4A1

(A) Western blot assay was performed to determine PTP4A1 protein level after transfection of WDR5/KAT2A siRNA, lentivirus harboring the full-length human *GCAWKR* sequence in SGC7901 cells (n = 3). (B) Luciferase reporter vector was generated by inserting the promoter region ($-2,000$ to 0 bp) of the PTP4A1 gene. The reporter vectors were then cotransfected into SGC7901 cells with *GCAWKR* or WDR5/KAT2A siRNA. Cells were harvested for luciferase activity assay. Results shown are the mean ± SD of triplicate determination from three independent experiments. *p < 0.05. (C) The PTP4A1 DNA was detected in the chromatin sample immunoprecipitated from SGC7901 cells using an antibody against WDR5, KAT2A, or p300. n = 3. (D) Real-time PCR of the ChIP samples shows the binding efficacy of WDR5 or KAT2A to the PTP4A1 gene promoter after transfection of WDR5/KAT2A siRNA or shRNA-*GCAWKR* in SGC7901 cells. Data are shown as the mean ± SD from three independent repeats. (E) The PTP4A1 DNA was detected in the chromatin sample immunoprecipitated from SGC7901 cells using an antibody against H3K4me3 or H3K9ac. (F) Real-time PCR of the ChIP samples shows the binding efficacy of H3K4me3, H3K9ac, or H3K27me3 to the PTP4A1 gene promoter after transfection of WDR5/KAT2A siRNA or shRNA-*GCAWKR* in SGC7901 cells. Data are shown as the mean ± SD from three independent repeats.

PTP4A1 overexpression (Figure S13B) markedly ameliorated the tumor-suppressive effect of *GCAWKR* silencing (Figures S13C and S13D). Thus, *GCAWKR* promotes GC development may partially depend on the upregulation of PTP4A1 expression.

DISCUSSION

The research on the underlying molecular mechanism of GC progression has identified some protein-coding genes[28–30] and miRNAs[31,32] as potential biomarkers and therapeutic targets. However, there has been a poor overlap between these biomarkers and prognostic indicators identified.[33–35] Thus, we suppose that it might to be feasible to establish a more accurate prognostic gene signature with various kinds of transcripts. In light of the notion that lincRNAs are abundantly expressed in mammalian cells and play a vital role in cell development and human disease, we hypothesize that lncRNAs might be potential biomarkers and prognostic indicators in GC. Up till now, several lncRNAs, including *GAPLINC*[14] and HOXA11-AS,[23] have been demonstrated to be involved in the development of GC. *GAPLINC* overexpression is associated with the poor survival of GC patients, and *GAPLINC* regulates CD44 as a molecular decoy for miR211-3p.[14] Patients with high HOXA11-AS expression had a shorter survival and poorer prognosis.[23] HOXA11-AS promotes proliferation and invasion of GC by scaffolding the chromatin modification factors PRC2, LSD1, and DNMT1.[23] FOXD2-AS1 was upregulated markedly in GC and positively correlated with a poor prognosis.[36] FOXD2-AS1 promoted GC tumorigenesis partly through EZH2 and LSD1 mediated EphB3 downregulation. Yet, only a very small portion of lncRNAs have been functionally characterized. lncRNAs were reported to bind to EZH2, LSD1, or DNMT.[23,36] However, most were focused on the histone-methyltransferase complexes; there were few studies on histone acetyltransferase. Yet, histone acetylation and methylation are both vital parts of histone modification. The finding of this study was consistent with our previous study.[14] It further highlights the importance of histone acetyltransferase and the universality of the pattern that histone acetylation and methylation might coordinately regulate the expression of target gene.

In this study, through the genomic analysis of our previous profiling data,[14] we identified a novel lncRNA (*GCAWKR*) that was markedly upregulated in GC tissues compared to adjacent normal tissues in two cohorts of patients with ISH and qRT-PCR analysis. High expression levels of *GCAWKR* was correlated with some clinicopathological factors, including larger tumor size, the presence of lymph node metastasis, advanced TNM stage, more frequent recurrence, and cancer-related mortality. These data suggest that *GCAWKR* could be a potential prognostic indicator of GC.

The gene ontology pathways enrichment found that *GCAWKR* had an impact on cell proliferation and cell migration. The bioinformatics analyses were functionally verified in *in vitro* and *in vivo* experimental models with loss-of-function and gain-of-function approaches. The molecular mechanisms of lncRNAs function can be diversified, and
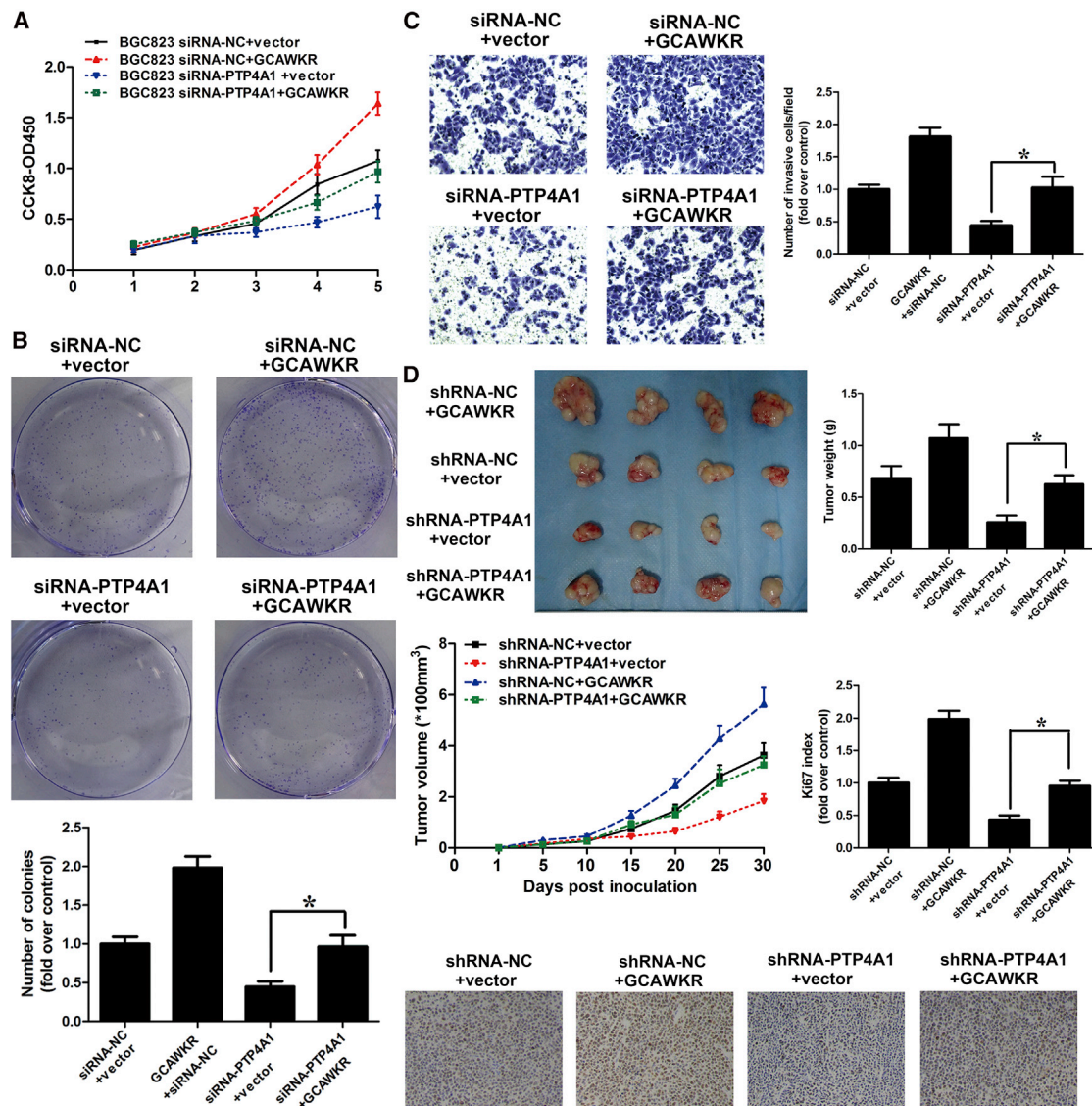
Figure 7. *GCAWKR* Regulates GC Development by Mediating PTP4A1 Expression

(A) CCK-8 assays showed that cell proliferation was inhibited in *GCAWKR*-overexpressing BGC823 cells after the cells were transfected with siRNA-PTP4A1. (B) Colony-formation assays showed that colony-formation ability was suppressed in *GCAWKR*-overexpressing BGC823 cells after the cells were transfected with siRNA-PTP4A1. (C) Effects of PTP4A1 knockdown on cell invasion in *GCAWKR*-overexpressing BGC823 cells in the presence of the anti-proliferative drug mitomycin C (MMC, 5 μM) treatment were determined using the transwell assay. *p < 0.05. (D) Top left, representative images of tumors formed in nude mice injected subcutaneously with BGC823 cells transfected with desired vector. Top right, tumor weights. Middle left, tumor growth curves. Bottom, representative images of IHC staining of Ki67 (original magnification, ×200). *p < 0.05.

lncRNAs located in the nucleus can guide and recruit chromatin-modifying complexes or transcriptional factors to the genomic loci, resulting in the activation or inactivation of target genes.[12] Here, we found that *GCAWKR* can function as a scaffold for WDR5 and KAT2A to regulate PTP4A1 expression transcriptionally. We verified the hypothesis with three lines of solid experimental evidence: (1) *GCAWKR* physically interacts with WDR5 and KAT2A; (2) *GCAWKR* knockdown or RNase treatment significantly suppressed the interaction between WDR5 and KAT2A; (3) *GCAWKR* knock-

down inhibited the recruitment of WDR5/KAT2A complexes to the promoter regions of target genes. In general, *GCAWKR* was capable of modulating the interaction between WDR5 and KAT2A, mediating the histone modification of target genes.

When exploring the underlying mechanisms of *GCAWKR*'s oncogenic role in GC, we found that PTP4A1 might be involved in this process with RNA sequencing. PTP4A1 was reported to be upregulated in GC and promotes tumor development.[18] Consistent with

the previous reports, we found that *GCAWKR* modulates the expression of PTP4A1, and PTP4A1 is the downstream effector of *GCAWKR*-mediated oncogenic effects. Also, RNA sequencing in *GCAWKR*-silencing cells demonstrated that some other genes that are involved in regulation of cell proliferation and migration could also be affected by *GCAWKR*, such as CDK1, CDC25B, CCND3, KLF6, and HOXB13. Thus, we do not rule out the possibility that other genes might take part in *GCAWKR*-mediated biological functions.

Our data suggest that *GCAWKR* is an oncogenic lncRNA that promotes the tumorigenesis of GC by functioning as a scaffold and recruiting histone-modifying complexes to target genes. The study suggests that *GCAWKR* might be the potential therapeutic target.

MATERIALS AND METHODS

Patient Samples

The study was under the censorship of the Clinical Research Committee of the Fudan University Shanghai Cancer Center (FUSCC). Written informed consent was obtained from all patients. Two cohorts of patients involving 165 GC tissues and paired normal tissues collected during 2008 and 2012 were obtained from the biobank of FUSCC. The clinicopathological features of the patients are in Tables S1 and S2. These data do not contain identity-related information. None of these patients had received preoperative chemo- or radio-therapy. All patients were staged according to the criteria of the WHO Classification of Tumors of the Digestive System, 2010 edition.

Bioinformatics Analysis

lncRNA profiling data are available via GEO: GSE50710. RNA sequencing data can be accessed via GSE112586. Detailed information can be found in the Supplemental Materials and Methods.

Cell Culture

The human gastric epithelial cell line GES-1 and five GC cell lines (SGC7901, BGC823, MKN45, HGC27, and AGS) were used in this study. These cell lines were purchased from the Health Science Research Resources Bank on September 2015. The cell lines were characterized by DNA fingerprinting, cell vitality detection, isozyme detection, and mycoplasma detection. The last cell characterization was performed on November 2017. Cells were cultured in DMEM (Gibco BRL) supplemented with 10% fetal bovine serum (FBS), 100 U/mL penicillin, 100 µg/mL streptomycin (Thermo Scientific), and 8 mg/L antibiotic tylosin tartrate against mycoplasma (Sigma-Aldrich, St. Louis, Missouri, USA) at 37°C in an atmosphere of 5% CO_2. The passage numbers for GES-1, SGC7901, BGC823, MKN45, HGC27, and AGS were 25, 30, 32, 37, 16, and 19, respectively.

RNA and Protein Extraction, Real-Time qPCR Analysis, and Western Blot Analysis

RNA and protein extraction, real-time qPCR analysis, and western blot analysis were performed.[12]

Subcellular Fractionation Analysis and 5′ and 3′ RACE Analysis

Subcellular fractionation analysis and 5′ and 3′ RACE analysis were performed as we described previously.[12]

Cell Viability, Colony Formation, and Transwell Assay

Cell viability was determined with the Cell Counting Kit 8 (CCK-8, Donjindo).[12] For colony formation assay, cells were seeded in 6-well plates at a density of 800 cells per well and incubated for 10 days. Colonies were fixed with ethanol for 20 min and stained with 0.1% crystal violet for 30 min. Transwell assays were utilized to assess cell-invasive ability with the Transwell system (Corning) precoated with Matrigel in the presence of anti-proliferative drug MMC.

RNA Pull-Down Assay, RNA IP, Coimmunoprecipitation, and ChIP

RNA pull-down assay and RNA IP were utilized to confirm the interaction between the lncRNA and the specific protein. Coimmunoprecipitation assay was used to verify the direct interaction between proteins. ChIP assay was employed to determine the binding of the chromatin-modifying complexes to the promoter regions of genes.

Plasmid Construction and Cell Transfection

Plasmid construction and cell transfections were performed as we described previously.[12]

ISH of *GCAWKR* and *In Vivo* Experiments

ISH was performed to evaluate the expression of *GCAWKR*. To further illustrate the role of *GCAWKR* in tumor growth, the *in vivo* tumor growth assay was performed.

4∼5-week-old male BALB/c nude mice were maintained under pathogen-free conditions in the Experimental Animal Centre of Xinhua Hospital. All animal experiments of laboratory animals were performed by the Guide for the Care and Use published by the US NIH (NIH publication number 85-23, revised 1996). Nude mice were injected subcutaneously into unilateral flank areas with GC cells (1×10^6) transfected with desired vector to establish tumors (n = 5 per group). Tumor growth was measured every 5 days for 30 days. Then, tumors were removed and weighed. The length (L) and width (W) were determined using calipers, and the tumor volumes were calculated using the following equation: $(L*W^2)/2$.

Statistical Analysis

All statistical analyses were performed using SPSS software (version 17.0, Chicago, IL). The difference between two or multiple groups was compared with Student's t test or one-way ANOVA test. The difference in *GCAWKR* levels in paired human samples was analyzed with the Wilcoxon test. The nonparametric Mann-Whitney-Wilcoxon test was utilized to assess the relationship between *GCAWKR* expression levels and clinicopathological factors. Spearman rank correlation test was used to test the correlation between *GCAWKR* and PTP4A1 expression levels. The survival curve was plotted with the Kaplan-Meier method, and the significance was calculated with the

log-rank test. The effect of clinicopathological factors on survival was determined with univariate and multivariate Cox proportional hazards models. All data are presented as the mean ± SD from three independent repeats. A two-sided p value less than 0.05 was considered to be statistically significant.

SUPPLEMENTAL INFORMATION

Supplemental Information includes eight tables, thirteen figures, and Supplemental Materials and Methods and can be found with this article online at https://doi.org/10.1016/j.ymthe.2018.09.002.

AUTHOR CONTRIBUTIONS

M.M., Y.Z., M.W., Y.H., and Y.X. acquired data, drafted the manuscript, and critically revised the manuscript for important intellectual content; M.M., M.W., and Y.Z. performed *in vitro* and *in vivo* assays; M.M. and Y.X. analyzed and interpreted data and statistical analysis; Y.R.H. and K.L. provided technical or material support; M.M., Y.R.H., and K.L. approved the final version of the manuscript.

CONFLICTS OF INTEREST

The authors have no conflicts of interest.

REFERENCES

1. Siegel, R.L., Miller, K.D., and Jemal, A. (2015). Cancer statistics, 2015. CA Cancer J. Clin. 65, 5–29.

2. Chen, W., Zheng, R., Baade, P.D., Zhang, S., Zeng, H., Bray, F., Jemal, A., Yu, X.Q., and He, J. (2016). Cancer statistics in China, 2015. CA Cancer J. Clin. 66, 115–132.

3. Dassen, A.E., Dikken, J.L., van de Velde, C.J., Wouters, M.W., Bosscha, K., and Lemmens, V.E. (2013). Changes in treatment patterns and their influence on long-term survival in patients with stages I–III gastric cancer in The Netherlands. Int. J. Cancer 133, 1859–1866.

4. Elimova, E., Wadhwa, R., Shiozaki, H., Sudo, K., Estrella, J.S., Badgwell, B.D., Das, P., Matamoros, A., Jr., Song, S., and Ajani, J.A. (2015). Molecular biomarkers in gastric cancer. J. Natl. Compr. Canc. Netw. 13, e19–e29.

5. Ponting, C.P., Oliver, P.L., and Reik, W. (2009). Evolution and functions of long non-coding RNAs. Cell 136, 629–641.

6. Qu, L., Ding, J., Chen, C., Wu, Z.J., Liu, B., Gao, Y., Chen, W., Liu, F., Sun, W., Li, X.F., et al. (2016). Exosome-Transmitted lncARSR Promotes Sunitinib Resistance in Renal Cancer by Acting as a Competing Endogenous RNA. Cancer Cell 29, 653–668.

7. Wang, P., Xue, Y., Han, Y., Lin, L., Wu, C., Xu, S., Jiang, Z., Xu, J., Liu, Q., and Cao, X. (2014). The STAT3-binding long noncoding RNA lnc-DC controls human dendritic cell differentiation. Science 344, 310–313.

8. Yang, F., Zhang, H., Mei, Y., and Wu, M. (2014). Reciprocal regulation of HIF-1α and lincRNA-p21 modulates the Warburg effect. Mol. Cell 53, 88–100.

9. Zhou, L., Sun, K., Zhao, Y., Zhang, S., Wang, X., Li, Y., Lu, L., Chen, X., Chen, F., Bao, X., et al. (2015). Linc-YY1 promotes myogenic differentiation and muscle regeneration through an interaction with the transcription factor YY1. Nat. Commun. 6, 10026.

10. Yuan, J.H., Yang, F., Wang, F., Ma, J.Z., Guo, Y.J., Tao, Q.F., Liu, F., Pan, W., Wang, T.T., Zhou, C.C., et al. (2014). A long noncoding RNA activated by TGF-β promotes the invasion-metastasis cascade in hepatocellular carcinoma. Cancer Cell 25, 666–681.

11. Cao, L., Zhang, P., Li, J., and Wu, M. (2017). *LAST*, a c-Myc-inducible long noncoding RNA, cooperates with CNBP to promote *CCND1* mRNA stability in human cells. eLife 6, e30433.

12. Ma, M.Z., Zhang, Y., Weng, M.Z., Wang, S.H., Hu, Y., Hou, Z.Y., Qin, Y.Y., Gong, W., Zhang, Y.J., Kong, X., et al. (2016). Long Noncoding RNA GCASPC, a Target of miR-17-3p, Negatively Regulates Pyruvate Carboxylase-Dependent Cell Proliferation in Gallbladder Cancer. Cancer Res. 76, 5361–5371.

13. Fang, S., Zhang, L., Guo, J., Niu, Y., Wu, Y., Li, H., Zhao, L., Li, X., Teng, X., Sun, X., et al. (2018). NONCODEV5: a comprehensive annotation database for long non-coding RNAs. Nucleic Acids Res. 46 (D1), D308–D314.

14. Sun, T.T., He, J., Liang, Q., Ren, L.L., Yan, T.T., Yu, T.C., Tang, J.Y., Bao, Y.J., Hu, Y., Lin, Y., et al. (2016). LncRNA GClnc1 Promotes Gastric Carcinogenesis and May Act as a Modular Scaffold of WDR5 and KAT2A Complexes to Specify the Histone Modification Pattern. Cancer Discov. 6, 784–801.

15. Zhou, C., Liu, G., Wang, L., Lu, Y., Yuan, L., Zheng, L., Chen, F., Peng, F., and Li, X. (2013). MiR-339-5p regulates the growth, colony formation and metastasis of colorectal cancer cells by targeting PRL-1. PLoS ONE 8, e63142.

16. Stephens, B., Han, H., Hostetter, G., Demeure, M.J., and Von Hoff, D.D. (2008). Small interfering RNA-mediated knockdown of PRL phosphatases results in altered Akt phosphorylation and reduced clonogenicity of pancreatic cancer cells. Mol. Cancer Ther. 7, 202–210.

17. Zhang, J.X., Mai, S.J., Huang, X.X., Wang, F.W., Liao, Y.J., Lin, M.C., Kung, H.F., Zeng, Y.X., and Xie, D. (2014). MiR-29c mediates epithelial-to-mesenchymal transition in human colorectal carcinoma metastasis via PTP4A and GNA13 regulation of β-catenin signaling. Ann. Oncol. 25, 2196–2204.

18. Dumaual, C.M., Sandusky, G.E., Soo, H.W., Werner, S.R., Crowell, P.L., and Randall, S.K. (2012). Tissue-specific alterations of PRL-1 and PRL-2 expression in cancer. Am. J. Transl. Res. 4, 83–101.

19. Marchese, F.P., and Huarte, M. (2014). Long non-coding RNAs and chromatin modifiers: their place in the epigenetic code. Epigenetics 9, 21–26.

20. Grebien, F., Vedadi, M., Getlik, M., Giambruno, R., Grover, A., Avellino, R., Skucha, A., Vittori, S., Kuznetsova, E., Smil, D., et al. (2015). Pharmacological targeting of the Wdr5-MLL interaction in C/EBPα N-terminal leukemia. Nat. Chem. Biol. 11, 571–578.

21. Trievel, R.C., Rojas, J.R., Sterner, D.E., Venkataramani, R.N., Wang, L., Zhou, J., Allis, C.D., Berger, S.L., and Marmorstein, R. (1999). Crystal structure and mechanism of histone acetylation of the yeast GCN5 transcriptional coactivator. Proc. Natl. Acad. Sci. USA 96, 8931–8936.

22. Li, Y., Wang, Z., Shi, H., Li, H., Li, L., Fang, R., Cai, X., Liu, B., Zhang, X., and Ye, L. (2016). HBXIP and LSD1 Scaffolded by lncRNA Hotair Mediate Transcriptional Activation by c-Myc. Cancer Res. 76, 293–304.

23. Sun, M., Nie, F., Wang, Y., Zhang, Z., Hou, J., He, D., Xie, M., Xu, L., De, W., Wang, Z., and Wang, J. (2016). LncRNA HOXA11-AS Promotes Proliferation and Invasion of Gastric Cancer by Scaffolding the Chromatin Modification Factors PRC2, LSD1, and DNMT1. Cancer Res. 76, 6299–6310.

24. Thomas, L.R., Foshage, A.M., Weissmiller, A.M., and Tansey, W.P. (2015). The MYC-WDR5 Nexus and Cancer. Cancer Res. 75, 4012–4015.

25. Kim, J.Y., Banerjee, T., Vinckevicius, A., Luo, Q., Parker, J.B., Baker, M.R., Radhakrishnan, I., Wei, J.J., Barish, G.D., and Chakravarti, D. (2014). A role for WDR5 in integrating threonine 11 phosphorylation to lysine 4 methylation on histone H3 during androgen signaling and in prostate cancer. Mol. Cell 54, 613–625.

26. Chen, L., Wei, T., Si, X., Wang, Q., Li, Y., Leng, Y., Deng, A., Chen, J., Wang, G., Zhu, S., and Kang, J. (2013). Lysine acetyltransferase GCN5 potentiates the growth of nonsmall cell lung cancer via promotion of E2F1, cyclin D1, and cyclin E1 expression. J. Biol. Chem. 288, 14510–14521.

27. Gruber, A.R., Lorenz, R., Bernhart, S.H., Neuböck, R., and Hofacker, I.L. (2008). The Vienna RNA websuite. Nucleic Acids Res. 36 (Suppl 2), W70–W74.

28. Zhou, Z., Ji, Z., Wang, Y., Li, J., Cao, H., Zhu, H.H., and Gao, W.Q. (2014). TRIM59 is up-regulated in gastric tumors, promoting ubiquitination and degradation of p53. Gastroenterology *147*, 1043–1054.

29. Chen, L., Min, L., Wang, X., Zhao, J., Chen, H., Qin, J., Chen, W., Shen, Z., Tang, Z., Gan, Q., et al. (2015). Loss of RACK1 Promotes Metastasis of Gastric Cancer by Inducing a miR-302c/IL8 Signaling Loop. Cancer Res. *75*, 3832–3841.

30. Wang, K., Liang, Q., Li, X., Tsoi, H., Zhang, J., Wang, H., Go, M.Y., Chiu, P.W., Ng, E.K., Sung, J.J., and Yu, J. (2016). MDGA2 is a novel tumour suppressor cooperating with DMAP1 in gastric cancer and is associated with disease outcome. Gut *65*, 1619–1631.

31. Shen, J., Xiao, Z., Wu, W.K., Wang, M.H., To, K.F., Chen, Y., Yang, W., Li, M.S., Shin, V.Y., Tong, J.H., et al. (2015). Epigenetic silencing of miR-490-3p reactivates the chromatin remodeler SMARCD1 to promote Helicobacter pylori-induced gastric carcinogenesis. Cancer Res. *75*, 754–765.

32. Sousa, J.F., Nam, K.T., Petersen, C.P., Lee, H.J., Yang, H.K., Kim, W.H., and Goldenring, J.R. (2016). miR-30-HNF4γ and miR-194-NR2F2 regulatory networks contribute to the upregulation of metaplasia markers in the stomach. Gut *65*, 914–924.

33. Ueda, T., Volinia, S., Okumura, H., Shimizu, M., Taccioli, C., Rossi, S., Alder, H., Liu, C.G., Oue, N., Yasui, W., et al. (2010). Relation between microRNA expression and progression and prognosis of gastric cancer: a microRNA expression analysis. Lancet Oncol. *11*, 136–146.

34. Li, X., Wu, W.K., Xing, R., Wong, S.H., Liu, Y., Fang, X., Zhang, Y., Wang, M., Wang, J., Li, L., et al. (2016). Distinct Subtypes of Gastric Cancer Defined by Molecular Characterization Include Novel Mutational Signatures with Prognostic Capability. Cancer Res. *76*, 1724–1732.

35. Busuttil, R.A., George, J., Tothill, R.W., Ioculano, K., Kowalczyk, A., Mitchell, C., Lade, S., Tan, P., Haviv, I., and Boussioutas, A. (2014). A signature predicting poor prognosis in gastric and ovarian cancer represents a coordinated macrophage and stromal response. Clin. Cancer Res. *20*, 2761–2772.

36. Xu, T.P., Wang, W.Y., Ma, P., Shuai, Y., Zhao, K., Wang, Y.F., Li, W., Xia, R., Chen, W.M., Zhang, E.B., and Shu, Y.Q. (2018). Upregulation of the long noncoding RNA FOXD2-AS1 promotes carcinogenesis by epigenetically silencing EphB3 through EZH2 and LSD1, and predicts poor prognosis in gastric cancer. Oncogene *37*, 5020–5036.